Analytical Model of Bracket Set Frame in Traditional Chinese Timber Structures

Qingshan Yang[1], Ke Liu[1(✉)], and Pan Yu[2]

[1] School of Civil Engineering, Chongqing University, Chongqing 400044, China
keliu@cqu.edu.cn

[2] College of Civil Engineering, Taiyuan University of Technology, Taiyuan 030024, China

Abstract. Bracket set frame (BSF) consists of two column-head bracket sets (CHBSs) and one beam (Tiaojianliang), CHBS consists of bearing blocks (Dou) and short beams (Gong), in a unique manner in traditional Chinese timber structures. The mechanical performances of a BSF is different from a rigid joint or hinge joint exhibiting the behavior of a semi-rigid joint. An analytical model of BSF along y-axis direction of a building is proposed. Based on the structural form of BSF, the analytical model of a BSF is composed of rotational spring elements representing the Mantousun (MTS), Dadou with mortise (DDM) and beam elements representing the beams (Gong, Fang and Tiaojianliang). The accuracy of this model is validated with a solid element model with the same geometric dimensions and mechanical parameters. Effects of the vertical load and section dimension of Tiaojianliang on the load resistance capacity of BSF are analyzed. Result suggests that the load resistance capacity of BSF will increase significantly with the vertical load increases. The load resistance capacity of BSF will decrease with the section dimension of Tiaojianliang decreases.

Keywords: Bracket Set Frame · Analytical Model · Rotational Spring Element · Vertical Load · Section dimension of Tiaojianliang

1 Introduction

A timber structure is very different from modern concrete or steel structure, and an introduction on its construction is beneficial before discussions on the existing problem in this analytical study. A typical traditional Chinese timber structure usually composes of three structural layers vertically, i.e., the roof frame layer (RFL), the bracket set layer (BSL) and the column frame layer (CFL), as shown in Fig. 1 (a), (b) and (c). The BSL consists of spatial bracket set frame (SBSF), bracket sets (BSs) and beams (Gong, Fang and Tiaojianliang) of different dimensions, as shown in Fig. 1 (b), (d), (e) and (f). BS is also named as Dou-Gong (DG), which consists of bearing blocks (Dou) and short beams (Gong), in a unique manner. The BSs may be broadly classified into three types according to their locations, i.e., the CHBS on top of a side column, the intermediate-column bracket set (ICBS) on a beam (E-Fang), and the corner bracket set (CBS) on top of a corner column.

Y. Endo and T. Hanazato (Eds.): SAHC 2023, RILEM Bookseries 46, pp. 301–311, 2024.
https://doi.org/10.1007/978-3-031-39450-8_25

The BSL includes spatial bracket set frame (SBSF) as shown in Fig. 1 (b) and (d). The SBSF includes BSF as shown in Fig. 1 (d) and (e). The BSF composes of two CHBSs and a long-span beam (Tiaojianliang) as shown in Fig. 1 (e) and (f).

In order to analyze the mechanical properties of traditional Chinese timber structures, it is necessary and efficient to establish their analytical model. Existing models on different components of the BSF are adopted. They included the analytical model of column foot [1], the analytical model of mortise-tenon (MT) connection [2, 3] and the analytical model of single bracket set [4]. The analytical model of BSF will be developed in this study.

This study proposes analytical model of BSF in traditional Chinese timber structures. BSF contains two CHBSs and one beam (Tiaojianliang). The CHBS contains MTS which is similar to mortise-tenon (MT) connection, the interface between Dadou and column head is similar to column foot (CF). Based on the above analysis and discussion, the analytical model of BSF is established. Based on the same geometric dimensions and mechanical parameters, the solid element (SE) model has been established to validate the accuracy of the analytical model. Finally, effects of vertical load and section dimension of Tiaojianliang on the load resistance capacity of BSF are discussed.

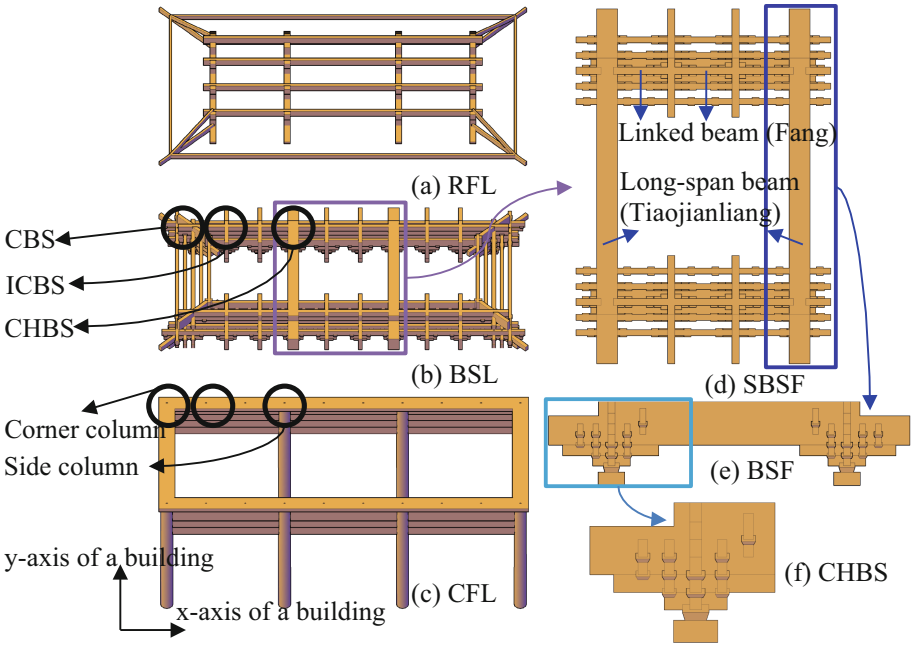

Fig. 1. BSF and its location and composition in a traditional Chinese timber structure.

2 The Proposed Analytical Model of BSF

2.1 Analysis of Structural Form of BSF

Vertical load such as the weight of tile, roof board and the snow load are firstly transferred to the RFL via flexural and shear actions, and then to the BSL in the form of concentrated forces. Horizontal loads such as wind load or earthquake load is transferred to the BSL by friction. Therefore, BSF is subjected to both horizontal and vertical loads, as shown in Fig. 2.

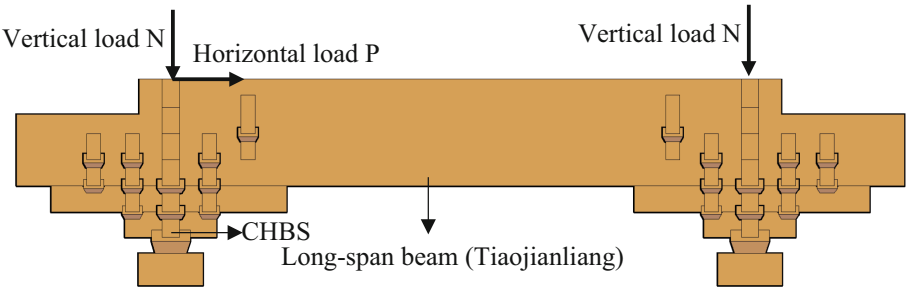

Fig. 2. BSF model along the y-axis of a building.

The schematic diagram of relative and absolute rotation in each layer of the CHBS when under vertical load and horizontal load along y-axis direction is shown in Fig. 3 (a). The fourth and fifth layers are joined by Tiaojianliang (Fig. 3 (b)), therefore, there are four interfaces in total, relative and absolute rotation may occur on the four interfaces, which could be simplified as rotational spring elements. Other part, i.e., the component between each interface and the Tiaojianliang could be simplified as beam elements as shown in Fig. 3 (b).

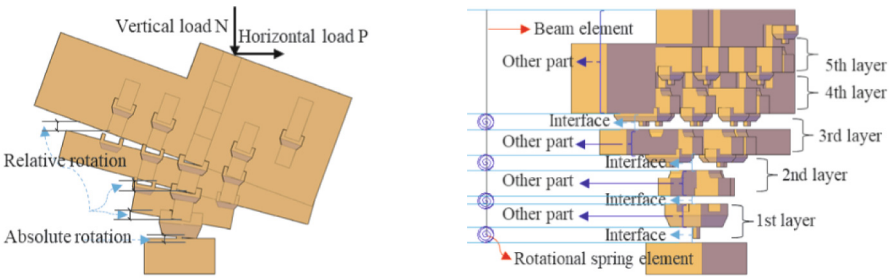

(a) relative and absolute rotation in each layer (b) Rotational spring element

Fig. 3. The schematic diagram of relative and absolute rotation in each layer and rotational spring element

As shown in Fig. 4 (a), the CHBS has distinct multiple layer construction. The structural decomposition in the y-axis direction is shown in the second column. According

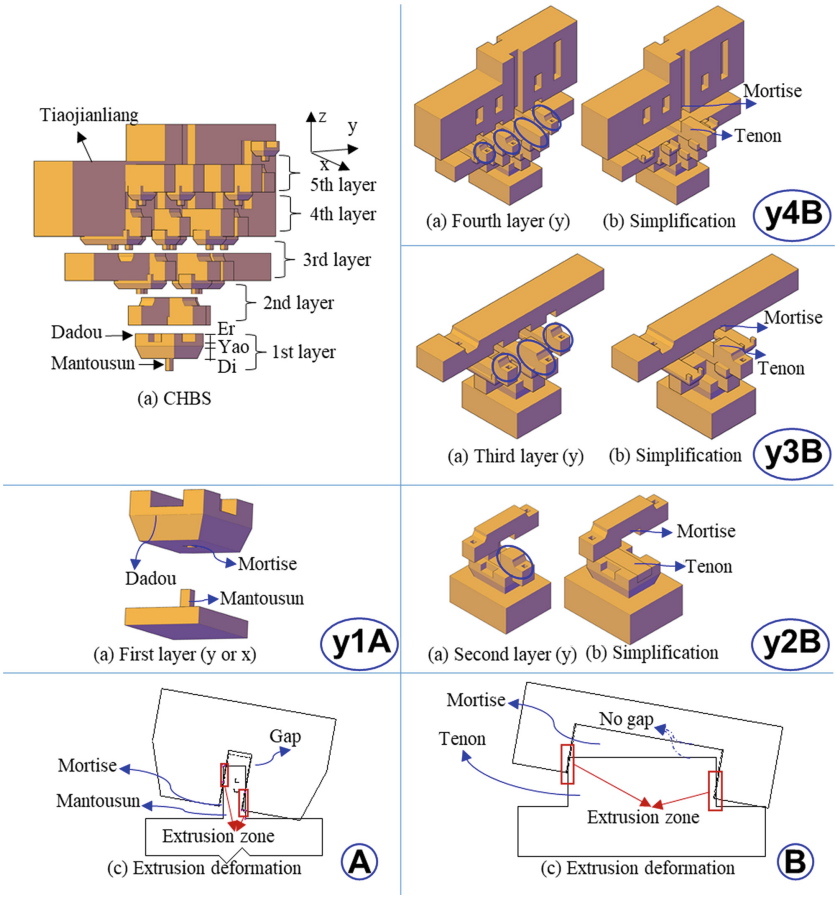

Fig. 4. Structural form and extrusion deformation of second layer of CHBS.

to different structural form, there are two kinds of rotational springs, named A and B respectively, as shown in the fourth line of Fig. 4, for example, the schematic diagram of structural form of the second layer in the y-axis direction is numbered y2B. Where (a) is the original structure, (b) is the simplified structure, (c) is the schematic diagram of extrusion or compression deformation, and so on in other cases.

The extrusion deformation relationship of first layer of CHBS is shown in Fig. 4 (A), which is referred as the analytical model of MTS and the analytical model of DDM as shown in Fig. 10, Fig. 11 and Fig. 12. The extrusion deformation relationship of the y-axis direction from second to fourth layer is shown in Fig. 4 (B), which is referred as the analytical model of MTS as shown in Fig. 10 and Fig. 11, the tenon in Fig. 4 (B) is similar to the MTS in Fig. 4 (A), the difference between them is whether there are gaps between the top of tenon or MTS and the upper components. Based on the analysis of structural form, the analytical model of BSF could be established according

to those rotational springs. And those rotational springs composed of analytical models of sub-joints. MTS and DDM could be called as sub-joints.

2.2 Analytical Model of BSF

The MTS model can be further simplified as a rotational spring element [2], the Dadou (Fig. 5 (a) and Fig. 10) with mortise model (DDm) can be further simplified as a rotational spring element [4], as shown in Appendix, they are the sub-joint analytical model of BSF. Based on the analysis of structural form in the above section, the analytical model of BSF contains these sub-joint analytical model, as shown in Fig. 5. BSF are simulated as rotational spring elements and beam elements in the axis of column head and Dadou. The interface between adjacent layers are modelled as rotational spring elements, the Gong, Fang and Tiaojianliang (Fig. 3 (b)) components have been modelled as beam elements. The simplified model of BSF is shown in Fig. 5. The stiffness matrix (Eq. (1)) of the BSF along the y-axis of a building is then obtained by assembling the stiffness matrices of different types of finite elements as Fig. 5, i.e., the Dadou, Mantousun and the column head (Fig. 3 (b)) is simplified as rotational spring element ①, the upper interfaces (second layer to fourth layer) of BSF (Fig. 3 (b)) are simplified as rotational spring element ③, ⑤, ⑦, the other parts are simplified as beam element ②, ④, ⑥, ⑧, ⑨, CHBS on the right and left in BSF are symmetrical.

$$K = \begin{bmatrix} k_{11}^{①} & k_{12}^{①} & 0 & \cdots & 0 \\ k_{21}^{①} & k_{22}^{①} + k_{22}^{②} & k_{23}^{②} & \cdots & 0 \\ 0 & k_{32}^{②} & k_{33}^{②} + k_{33}^{③} & \cdots & 0 \\ \vdots & \vdots & \vdots & \ddots & \vdots \\ 0 & 0 & 0 & \cdots & k_{1818}^{⑰} \end{bmatrix} \tag{1}$$

where, K donates the stiffness matrix of BSF; $k_{ij}^{⑥}$ donates one of the four submatrices of the stiffness matrix of element e; i and j are the node numbers of element e. The load-displacement relationship can be obtained as Eq. (2)

$$F = K\Delta \tag{2}$$

where, F and Δ donate the load and displacement, respectively.

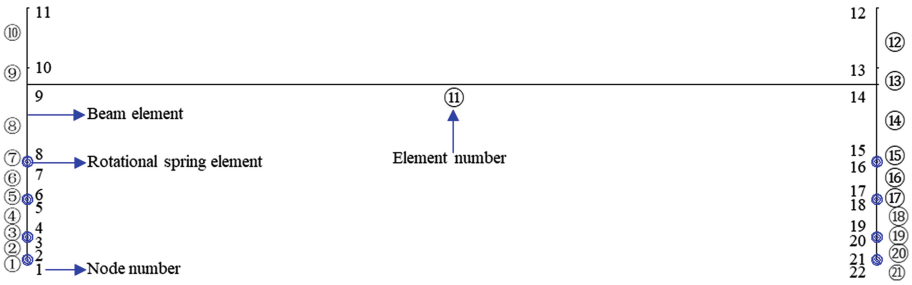

Fig. 5. Simplified rotational spring model of BSF.

3 Validation of Analytical Model

3.1 Solid Element Model of BSF

The BSF model is established in CAD (see Fig. 2), which only have geometric information and could not be analyzed mechanically. Then they have been imported into ABAQUS (see Fig. 6) to input mechanical parameters, interaction, boundary conditions and load condition, etc. 8-node hexahedral finite elements (element C3D8R) is adopted and the mesh of solid element of BSF is shown in Fig. 7. The red coordinates are the local coordinates, and the black coordinates are the global coordinates. The parallel-to-grain direction (the x-axis in the red coordinate system) of the Gong and beam components is perpendicular to the z-axis (in the black coordinate system) as shown in Fig. 6. The parallel-to-grain direction of other components is parallel to the z-axis as shown in Fig. 6 [5]. One step further, the BSF model is calculated and solved in ABAQUS. Finally, the result is output from ABAQUS for mechanical analysis.

Fig. 6. Assembly of solid element of BSF.

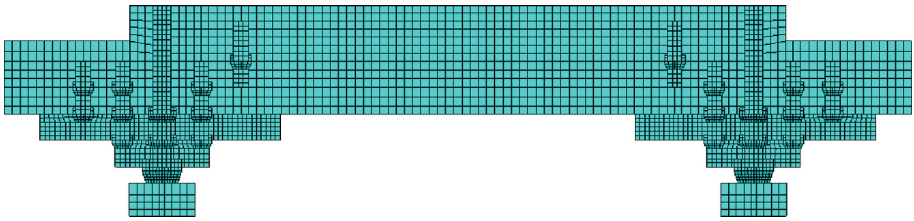

Fig. 7. Mesh of solid element of BSF.

3.2 Validation of Analytical Model of BSF

The load-displacement relationship of the BSF is in good agreement with that from the solid element model as shown in Fig. 8. This indicates the rationality of the analytical model.

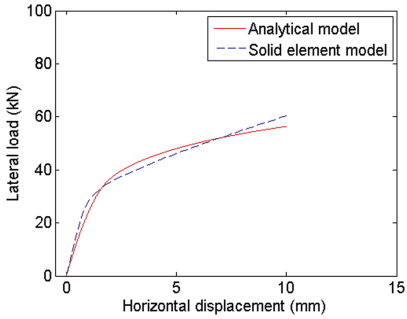

Fig. 8. The load-displacement relationship of BSF.

4 Mechanical Performances of BSF

4.1 The Effect of Vertical Load on the Load Resistance Capacity of BSF

Heavy RFL is one of the remarkable features of traditional Chinese timber structures, as it plays an important role in energy dissipation [6] during a seismic event. Vertical loads with a value of 10kN, 20kN, 30kN 40kN and 50kN are applied separately to the top surface of BSF as shown in Fig. 2 respectively, and the load-displacement curve is shown in Fig. 9 (a). The load resistance capacity increases significantly as the vertical load increases, which suggests a heavy RFL would contribute notably to the load resistance capacity of the BSF.

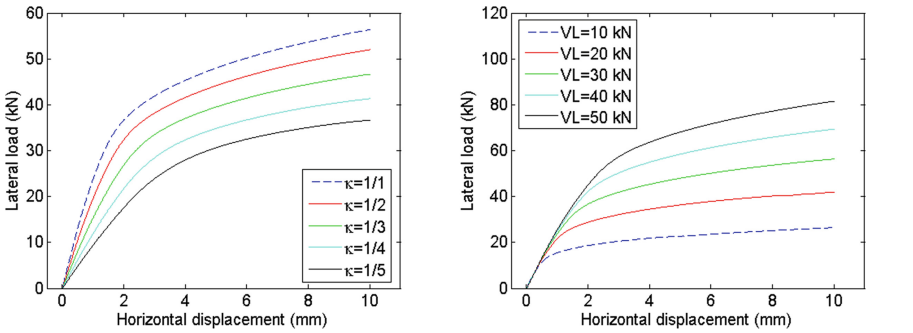

(a) The effect of vertical load (b) The effect of section dimension of Tiaojianliang

Fig. 9. The load-displacement relationship of BSF.

4.2 The Effect of Section Dimension of Tiaojianliang on the Load Resistance Capacity of BSF

The original section dimension of Tiaojianliang is taken as standard and referred as coefficient of section dimension κ. . Considering the large section size of the beam

(Fig. 1 (d), (e) and Fig. 2), the gradient reduction of section area is taken as the variable. $\kappa = 2$ means that the width and height of the section are $\sqrt{2}$ times of the original width and height respectively, and so on in other cases. It could be concluded that the load resistance capacity of BSF will decrease with the section dimension of Tiaojianliang decreases from Fig. 9 (b).

5 Conclusion

Owning to the mechanical performances of semi-rigid joint of BSF, a rotational spring model is the core part of analytical model of BSF. The main conclusions of this study are summarized as follow.

1. The analytical model of BSF considering the interaction between the upper and lower components, layer number and components assembly method in the meantime is proposed.
2. Load resistance capacity of BSF increases significantly as vertical load increases, which suggests heavy RFL plays an important structural function in the resistance to lateral load.
3. The load resistance capacity of BSF will decrease with the section dimension of Tiaojianliang decreases.

Acknowledgments. The work was supported the 111 project of the Ministry of Education and the Bureau of Foreign Experts of China (No. B18062), National Natural Science Foundation of China (51720105005) and Chongqing Science and Technology Bureau (cstc2020yszx-jcyjX0007).

Appendix

When the BSF or CHBS under horizontal and vertical loads, the relative rotation would occur, the bending moment is consistent of two parts, i.e., the first part is extrusion deformation between Dadou and Mantousun, the second part is the compressive deformation between Dadou and column head, as shown in Fig. 10. The derivation of the two parts is referenced from [4].

The bending moment of first part is shown [4] as Eq. (3), and the extrusion deformation volume is in Eq. (4) and (5).

$$M_1 = \left(L_{c1} + \mu cos\theta L_{f1}\right)\frac{E_R}{l_t}V_{t1} + \left(L_{c2} + \mu cos\theta L_{f2}\right)\frac{E_R}{l_t}V_{t2} \tag{3}$$

$$V_{t1} = S_{\Delta ABC}w_t = \frac{w_t}{2}\left(\frac{BC^2}{tan\theta}\right) \tag{4}$$

$$V_{t2} = \frac{w_t}{2}\left(\frac{EF^2}{tan\theta}\right) + w_t\left(\frac{1 - e^{-3\alpha l_t/2}}{\alpha}\right)EF \tag{5}$$

where, μ is the frictional coefficient. θ is the rotation angle. L_{c1}, L_{c2}, L_{f1} and L_{f2} are the arm of force corresponding to P_{c1}, P_{c2}, P_{f1} and P_{f2}. l_t and w_t are the length and

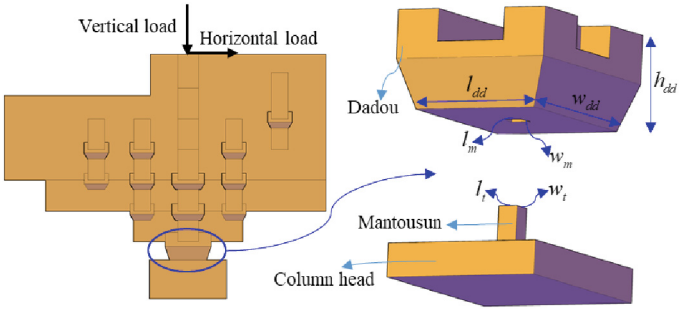

Fig. 10. The extrusion deformation between Dadou and Mantousun.

width of tenon. E_R is elastic modulus of 'Radial' directions of the timber member. V_{t1} and V_{t2} are the extrusion deformation volume on the left and right part of Mantousun. The diagram of each symbol is shown in Fig. 10 and Fig. 11.

The bending moment of second part is between Dadou and column head [4], there are four working states as shown in Fig. 12. The bending moment and the critical rotational angle of each working state are shown in Eq. (6) to (12).

$$M_{2-1} = \frac{E_L\left(w_{dd}l_{dd}^3 - w_m l_m^3\right)}{12h_{dd}}tan\theta \tag{6}$$

$$\theta_1 = arctan\left(\frac{2h_{dd}N_{DG}}{E_L l_{dd}\left(l_{dd}w_{dd} - l_m w_m\right)}\right) \tag{7}$$

$$M_{2-2} = -\frac{E_L w_m l_m^3}{12h_{dd}}tan\theta + \frac{E_L w_{dd} l_{dd}}{4h_{dd}}h_1^2 cot\theta - \frac{E_L w_{dd}}{6h_{dd}}h_1^3(cot\theta)^2 \tag{8}$$

$$\theta_2 = arctan\left(\frac{8h_{dd}N_{DG}}{E_L\left(-4w_m l_m^2 + w_{dd}\left(l_{dd} + l_m\right)^2\right)}\right) \tag{9}$$

$$\begin{aligned} M_{2-3} = &-\frac{E_L(l_{dd} + 2l_m)w_m(l_{dd} - l_m)^2}{48h_{dd}}tan\theta + \frac{E_L w_m\left(l_{dd}^2 - l_m^2\right)}{8h_{dd}}h_1 \\ &+\frac{E_L l_{dd}(w_{dd} - w_m)}{4h_{dd}}h_1^2 cot\theta - \frac{E_L(w_{dd} - w_m)}{6h_{dd}}h_1^3(cot\theta)^2 \end{aligned} \tag{10}$$

$$\theta_3 = arctan\left(\frac{8h_{dd}N_{DG}}{E_L w_{dd}\left(l_{dd} - l_m\right)^2}\right) \tag{11}$$

$$M_{2-4} = \frac{N_{DG}l_{dd}}{2} - \frac{1}{3}\sqrt{\frac{2N_{DG}^3 h_{dd}}{E_L w_{dd}}}\sqrt{cot\theta} \tag{12}$$

where, E_L is elastic modulus of 'Longitudinal' directions of the timber member. l_{dd}, w_{dd} and h_{dd} are the length, width and height of Dadou. l_m and w_m are the length and width of mortise. N_{DG} is the vertical load which is applied to the top surface of CHBS in BSF. The diagram of each symbol is shown in Fig. 10.

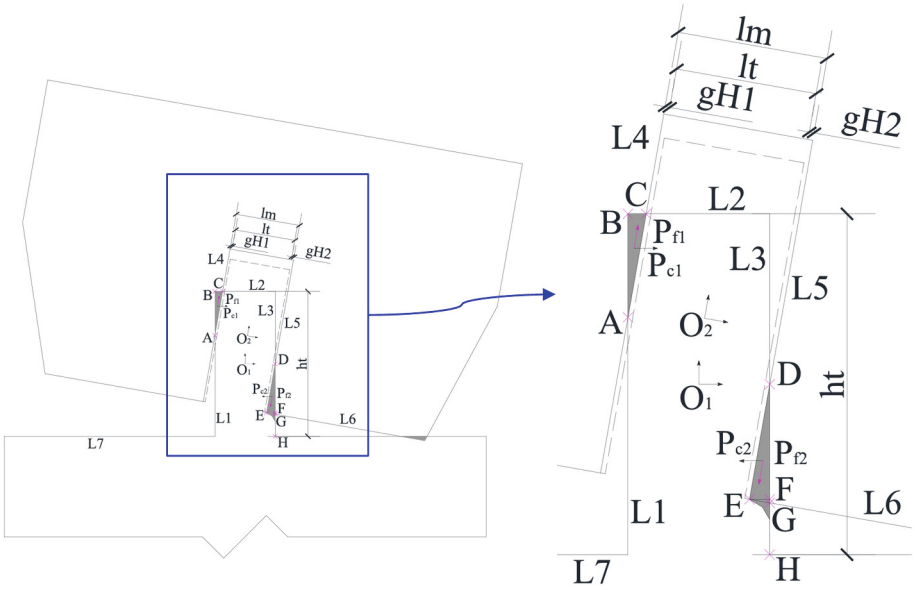

Fig. 11. The schematic diagram of plan extrusion deformation between Dadou and Mantousun.

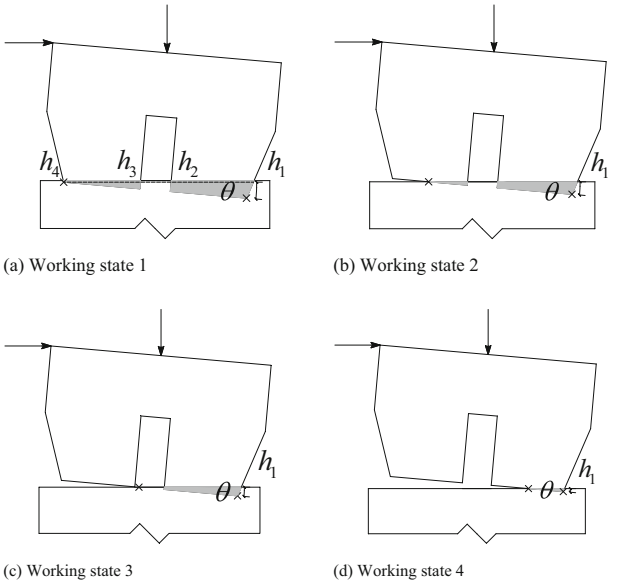

Fig. 12. The load-displacement relationship of BSF.

The bending moments in the four working states can be summarized as Eq. (13).

$$M_2 = \begin{cases} M_{2-1}0 \leq \theta < \theta_1 \\ M_{2-2}\theta_1 \leq \theta < \theta_2 \\ M_{2-3}\theta_2 \leq \theta < \theta_3 \\ M_{2-4}\theta_3 \leq \theta \end{cases} \tag{13}$$

The total bending moment is the sum of M_1 and M_2, and taking the derivative of the bending moments with respect to rational angle θ, the rotational spring stiffness K could be obtained.

References

1. He, J., Wang, J.: Theoretical model and finite element analysis for restoring moment at column foot during rocking. J. Wood Sci. **64**(2), 97–111 (2017). https://doi.org/10.1007/s10086-017-1677-5
2. Yang, Q., Yu, P., Law, S.: Load resisting mechanism of the mortise-tenon connection with gaps under in-plane forces and moments. Eng. Struct. **219**, 110755 (2020)
3. He, J., Yu, P., Wang, J., Yang, Q., Han, M., Xie, L.: Theoretical model of bending moment for the penetrated mortise-tenon joint involving gaps in traditional timber structure. J. Build. Eng. **42**, 103105 (2021)
4. Yu, P., Yang, Q., Law, S., Liu, K.: Seismic performances assessment of heritage timber frame based on energy dissipation. J. Build. Eng. **56**, 104762 (2022)
5. Yeo, S., Komatsu, K., Hsu, M., Que, Z.: Mechanical model for complex brackets system of the Taiwanese traditional Dieh-Dou timber structures. Adv. Struct. Eng. **19**(1), 65–85 (2016)
6. Meng, X., Li, T., Yang, Q.: Experimental study on the seismic mechanism of a full-scale traditional Chinese timber structure. Eng. Struct. **180**, 484–493 (2019)